Supplementary material

METHODS

Mouse models

All animal procedures were approved by The Ohio State University Institutional Animal Care and Use Committee and conformed to the Guide for the Care and Use of Laboratory Animals published by the US National Institutes of Health (NIH Publication No. 85-23, revised 1996). Experiments were performed using two to four month-old male mice. Wild-type (C57BL/6J, WT) and NADPH oxidase type 2 knockout mice (NOX2KO, B6.129S6-Cybb^{tm1Din}/J; stock no. 002365)[1] were purchased from the Jackson Laboratory (Bar Harbor, ME). NOX2KO mice were inbred on the C57BL/6 background. Inducible mitochondrial superoxide dismutase (SOD2) overexpression mice[2] had a mixed NMRI (outbred), C57BL/6 and DBA/2 background. SOD2 overexpression was induced by administration of doxycycline (DOX) in the diet for at least 14 days (SOD2Dox+). In RyR2 knock-in mice, RyR2-S2814A (inbred on the C57BL/6 background),[3] serine at 2814 is replaced with alanine to prevent phosphorylation of RyR2 at this site.

Myocyte isolation

Mouse ventricular myocytes were isolated following standard procedures. Briefly, mice were anesthetized with isoflurane (3%) while depth of anesthesia was assessed by testing of foot reflexes, and were then sacrificed by exsanguination. Mouse hearts were cannulated and perfused with a modified Langendorff system in 37°C Ca^{2+}-free Tyrode solution containing (mM): 140 NaCl, 5.4 KCl, 0.5 $MgCl_2$, 10 HEPES, and 5.6 glucose (pH 7.3). After 5 minute wash, hearts were transferred to a digesting enzyme solution containing 2 μM Ca^{2+} Tyrode with 0.24 U Liberase TH Research Grade (Roche). When the heart became soft and pale, the ventricle was

cut, placed into bovine serum albumin solution, and agitated to dissociate myocytes. The ventricular myocytes were collected and used within 3.5 hours of isolation.

Confocal microscopy

Intracellular Ca^{2+} cycling and ROS production in isolated ventricular myocytes were monitored by an Olympus Fluoview 1000 confocal microscope using the Ca^{2+}- and ROS-sensitive indicators Fluo-3 AM (10 μM) and CM-H_2DCFDA AM (10 μM) as previously described.[4] Cells were loaded with the dyes for 25 to 30 minutes at room temperature for Fluo-3 and 37°C for CM-H_2DCFDA. Loaded cells were excited with the 488 nm line of an argon laser, and emission was collected at 500-600 nm for Fluo-3 and 500-560 nm for CM-H_2DCFDA. Myocytes were paced at 0.3-2 Hz using extracellular platinum electrodes and analyzed at 0.3 Hz. Experiments were performed either at room temperature or 37°C (Supplement fig. 10) in 1.8 mM Ca^{2+} Tyrode. To test the proarrhythmic effects of cardiac glycosides, myocytes were exposed to digitoxin (DGT). In some experiments, myocytes were pretreated with a general blocker of NADPH oxidase, diphenyliodonium chloride (DPI, 50 μM); a potent inhibitor of mitochondria permeability transition pore, cyclosporin A (CsA, 10 μM); or a selective CaMKII blocker, KN93 (1 μM). To examine the involvement of phosphatidylinositol 3 kinase (PI3K), protein kinase C and mitochondrial K_{ATP} channel in DGT-induced ROS production, LY294002 (LY, 10 μM) Bisindolylmaleimide I (BIM, 100 nM), εV1-2 (100 nM) and 5-hydroxydecanoate (5-HD, 200 μM) were used, respectively. Effects of DGT on NKA's Na^+ transport activity were recorded by the Na^+ indicator, sodium green (6.5 μM, 60 mins), with peak excitation and emission wavelengths 507 nm and 532 nm. For mitochondrial membrane potential measurement, cells were incubated with 75 nM tetramethylrhodamine ethyl ester (TMRE) for 15 to 20 minutes at 37°C. Excitation wavelength of TMRE was 543 nm and emission wavelength was between 570 and 650 nm. Data were normalized to the minimum TMRE fluorescence signal in the presence of 3 μM mitochondrial uncoupler, carbonyl cyanide p-(trifluoromethoxy) phenylhydrazone (FCCP).

Western Blotting

Samples were prepared from Langendorff-perfused intact mouse hearts with 1.8 mM Ca^{2+} Tyrode solution in the presence or absence of 150 nM DGT at 37°C for 30 minutes, and then samples were instantly frozen in liquid nitrogen. For ox-CaMKII assay, equal quantities of ventricular lysates were analyzed by SDS-PAGE and immunoblotting. Equal protein loading was verified by analyzing Coomassie and Ponceau stains of gels and blots.[5] Additionally, any slight differences in protein loading were corrected using a mouse monoclonal antibody to GAPDH (Fitzgerald). For RyR2 phosphorylation blots, cardiac homogenates were prepared from the fresh-frozen hearts, and protein concentrations were determined by Bradford assay. 60 µg cardiac homogenates were subjected to 4% to 15% SDS-PAGE, and blotted onto nitrocellulose membranes.[6] The blots were developed with Super Signal West Pico (PIERCE) and quantified using ImageJ software. For the RyR2 oxidation assay, samples were prepared as mentioned above and incubated with 0.5 mM thiol reactive maleimide-activated DyLight 650 (Pierce). Sample preparation and labeling were conducted with minimal sample exposure to light. Resultant labeled homogenates were then subjected to fractionation on a 3% to 8% Tris-Acetate Gel electrophoresis and free (non-oxidized) cysteines visualized in gel on a Typhoon 9410 imaging system (GE Healthcare). Following imaging gels were transferred and total RyR2 determined by sequential fluorescent Western blot. Resultant gel images were quantified using ImageQuant TL 7.0 (GE Healthcare) and the RyR free thiol levels normalized to total RyR amount.

Reagents

Anti-ox-CaMKII antiserum was developed and validated, as described.[5] Antibodies detecting RyR2 phosphorylation at Ser 2808 and Ser 2814 were from Badrilla Ltd, with catalog numbers A010-30P and A010-31P, respectively. Anti-RyR2 were from Thermo Scientific (Pierce antibodies), with catalog number MA3-916. Antibodies detecting PLB phosphorylation at Ser 16

and Thr 17 were from Upstate (07-052) and Santa Cruz Biotechnology (sc-17024-R), respectively. Anti-GAPDH was from Abcam (ab9483). Other chemicals were obtained from Sigma (St. Louis, MO) or Calbiochem (La Jolla, CA), and fluorescent indicators were purchased from Invitrogen (Grand Island, NY) or Thermo Scientific (Rockford, IL).

Statistical Analysis

Data are presented as mean ± SE. Statistical analyses were performed using ANOVA with Tukey's post hoc test. A level of $P < 0.05$ was accepted as statistically significant.

REFERENCES

1. Pollock JD, Williams DA, Gifford MAC, Li LL, Du X, Fisherman J, Orkin SH, Doerschuk CM, Dinauer MC. Mouse model of X–linked chronic granulomatous disease, an inherited defect in phagocyte superoxide production. *Nat Genet*. 1995;**9**:202–209.

2. Usui S, Komeima K, Lee SY, Jo Y-J, Ueno S, Rogers BS, Wu Z, Shen J, Lu L, Oveson BC, Rabinovitch PS, Campochiaro PA. Increased Expression of Catalase and Superoxide Dismutase 2 Reduces Cone Cell Death in Retinitis Pigmentosa. *Mol Ther*. 2009;**17**:778–786.

3. Chelu MG, Sarma S, Sood S, Wang S, Oort RJ van, Skapura DG, Li N, Santonastasi M, Müller FU, Schmitz W, Schotten U, Anderson ME, Valderrábano M, Dobrev D, Wehrens XHT. Calmodulin kinase II-mediated sarcoplasmic reticulum Ca2+ leak promotes atrial fibrillation in mice. *J Clin Invest*. 2009;**119**:1940–1951.

4. Ho H-T, Stevens SCW, Terentyeva R, Carnes CA, Terentyev D, Györke S. Arrhythmogenic adverse effects of cardiac glycosides are mediated by redox modification of ryanodine receptors. *J Physiol*. 2011;**589**:4697–4708.

5. Erickson JR, Joiner MA, Guan X, Kutschke W, Yang J, Oddis CV, Bartlett RK, Lowe JS, O'Donnell SE, Aykin-Burns N, Zimmerman MC, Zimmerman K, Ham A-JL, Weiss RM, Spitz DR, Shea MA, Colbran RJ, Mohler PJ, Anderson ME. A Dynamic Pathway for Calcium-Independent Activation of CaMKII by Methionine Oxidation. *Cell*. 2008;**133**:462–474.

6. Belevych AE, Terentyev D, Terentyeva R, Ho H-T, Gyorke I, Bonilla IM, Carnes CA, Billman GE, Györke S. Shortened Ca2+ Signaling Refractoriness Underlies Cellular Arrhythmogenesis in a Postinfarction Model of Sudden Cardiac Death. *Circ Res*. 2012;**110**:569–577.

FIGURE LEGENDS

Supplement 1: DGT-dependent alterations in Ca^{2+} handling in WT myocytes. A, representative line-scan images (top) and time-dependent profiles (bottom) of intracellular Ca^{2+} handling under control condition and in the presence of 150 nM DGT, 50 μM DPI + 150 nM DGT, and 10 μM CsA + 150 nM DGT, as indicated. **B,** pooled data for the amplitude of Ca^{2+} transients and frequency of SCWs in the presence of different concentrations of the drug. **C,** pooled data for the amplitude of Ca^{2+} transients and frequency of SCWs in control and in the presence of 150 nM DGT with the inhibitors (N= 5 to 22). (Note different scales for SCW frequency in B and C). *P<0.05 vs control.

Supplement 2: SR Ca^{2+} load. Bar graphs for SR Ca^{2+} contents in WT and genetically altered (NOX2KO, RyR-S2814A and SOD2) myocytes under control condition and in the presence of 150 nM DGT measured by application of 20 mM caffeine (N= 12 to 34). *P<0.05 vs control.

Supplement 3: Intracellular [Na^{+}]. Bar graphs for relative sodium green fluorescence (Na^{+} indicator) in WT and NOX2KO myocytes (N= 3). *P<0.05 vs data without DGT.

Supplement 4: CaMKII autophosphorylation. A,B representative western blots and normalized pooled data of CaMKII autophosphorylation level at Thr 287 from ventricular tissue prepared from WT and NOX2KO mice with or without 150 nM DGT (N= 4). Data were normalized to control (without DGT) on the same gel. *P<0.05 vs data without DGT.

Supplement 5: PLB phosphorylation. A,B representative western blots and normalized pooled data of phosphorylation level at Ser 16 (PKA-dependent) and Thr 17 (CaMKII-dependent) of phospholamban (PLB) from WT and NOX2KO myocytes with or without 150 nM

DGT (N= 3). Data were normalized to control (without DGT) on the same gel. *P<0.05 vs data without DGT.

Supplement 6: Oxidation of RyR2 in WT and RyR-S2814A hearts. A, representative simultaneous detection of free thiol and total RyR2 levels in WT and RyR-S2814A hearts. The left panel shows the free thiol content as detected by thiol reactive maleimide-activated DyLight 650 fluorescent labeling in WT and RyR-S2814A samples. The middle panel shows the sequential fluorescent Western detection of total RyR2 by RyR2-specific antibody. The right panel shows the merge of free thiol (blue) and total RyR2 signals (green). **B,** bar graphs of relative free thiol contents normalized to total RyR2 (N= 3 to 4). Data were normalized to control (without DGT) on the same gel. *P<0.05 vs data without DGT.

Supplement 7: The effects of DGT and DPI on Ca^{2+} wave frequency at room temperature vs 37°C. Representative line-scan image and time-dependent profile of intracellular Ca^{2+} handling in the presence of 150 nM DGT at 37°C (left), and pooled data for frequency of SCWs in control and in the presence of 150 nM DGT with 50 μM DPI at room temperature and at 37°C (right). The arrhythmogenic effects of DGT were even more pronounced at 37°C than at room temperature and were similarly inhibited by DPI. These results along with those of our biochemical protein phosphorylation- and oxidation assays (fig. 4 and supplemental fig. 5, 6, 7) suggest that our findings are applicable to “physiological” 37°C (N= 4 to 5). *P<0.05 vs data without DGT.

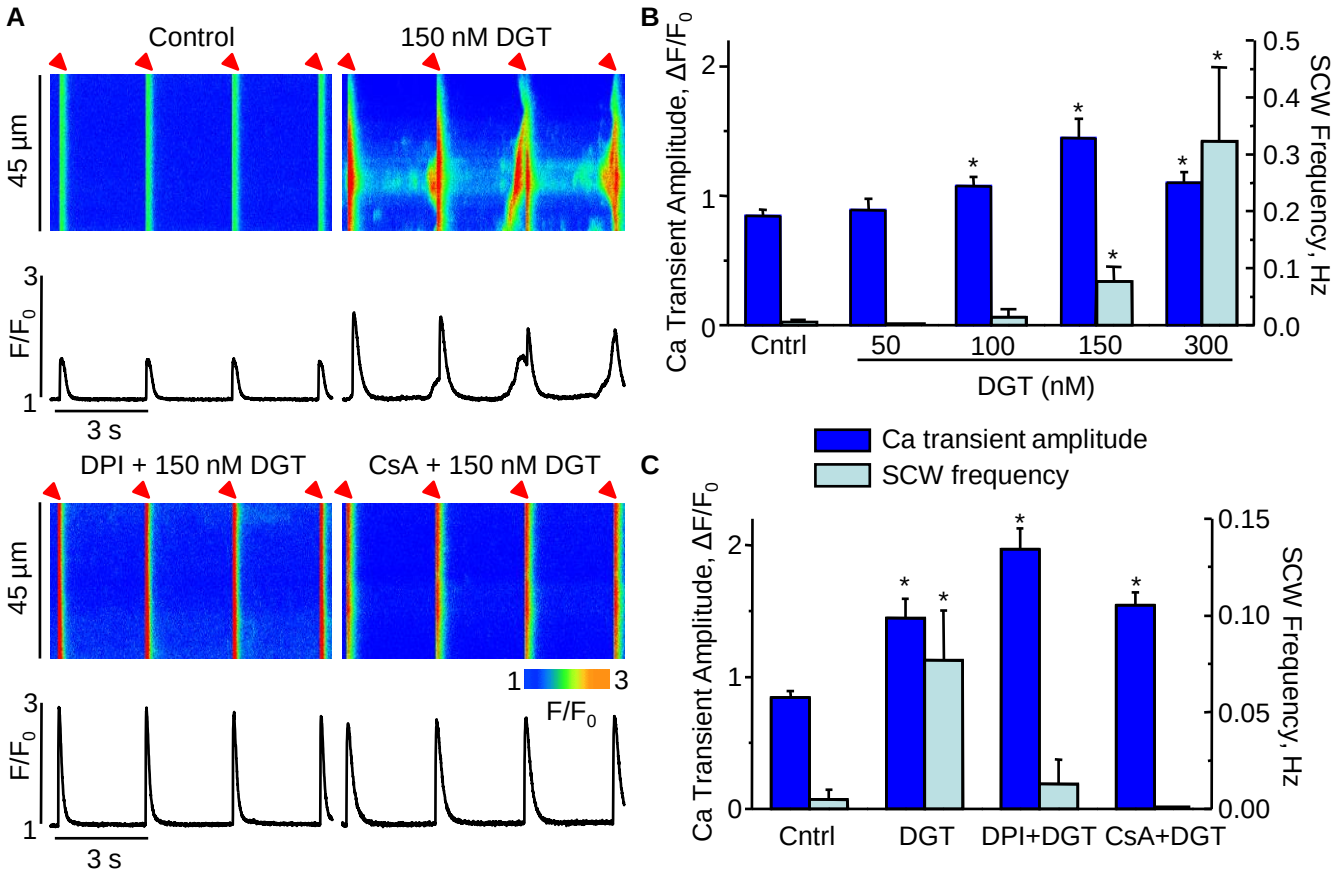

Supplement 1: DGT-dependent alterations in Ca^{2+} handling in WT myocytes. A, representative line-scan images (top) and time-dependent profiles (bottom) of intracellular Ca^{2+} handling under control condition and in the presence of 150 nM DGT, 50 µM DPI + 150 nM DGT, and 10 µM CsA + 150 nM DGT, as indicated. **B,** pooled data for the amplitude of Ca^{2+} transients and frequency of SCWs in the presence of different concentrations of the drug. **C,** pooled data for the amplitude of Ca^{2+} transients and frequency of SCWs in control and in the presence of 150 nM DGT with the inhibitors (N= 5 to 22). (Note different scales for SCW frequency in B and C). *P<0.05 vs control.

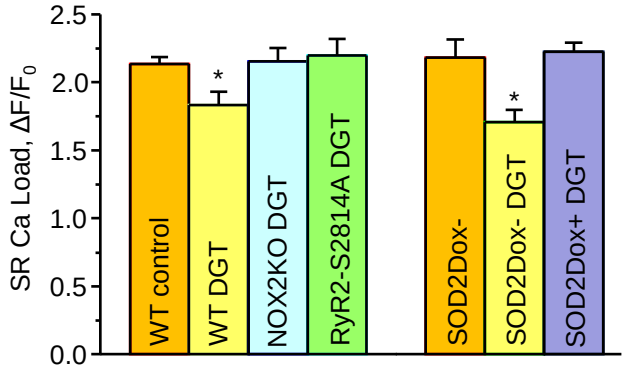

Supplement 2: SR Ca^{2+} load. Bar graphs for SR Ca^{2+} contents in WT and genetically altered (NOX2KO, RyR-S2814A and SOD2) myocytes under control condition and in the presence of 150 nM DGT measured by application of 20 mM caffeine (N= 12 to 34). *P<0.05 vs control.

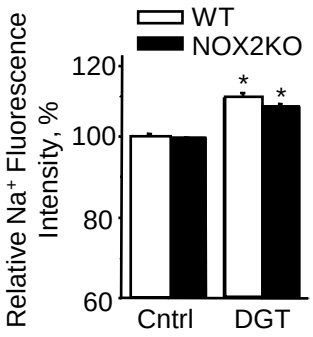

Supplement 3: Intracellular [Na^+]. Bar graphs for relative sodium green fluorescence (Na^+ indicator) in WT and NOX2KO myocytes (N= 3). *P<0.05 vs data without DGT.

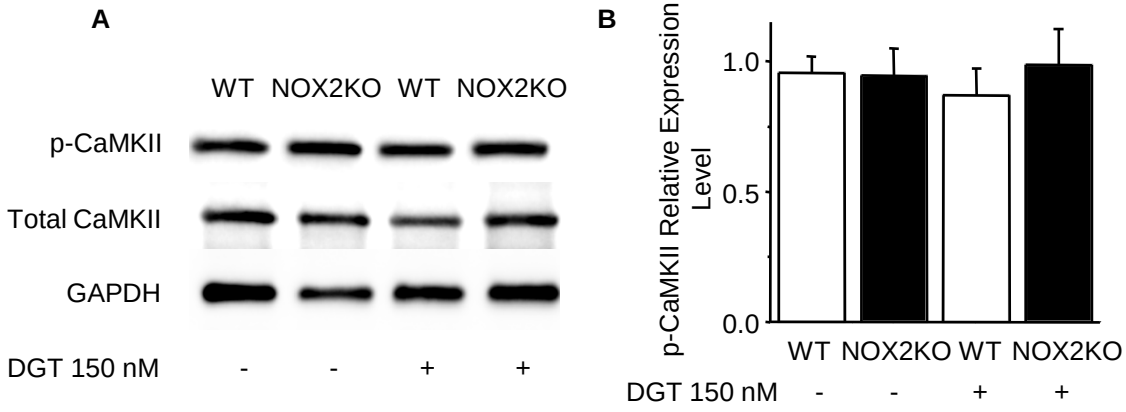

Supplement 4: CaMKII autophosphorylation. A,B representative western blots and normalized pooled data of CaMKII autophosphorylation level at Thr 287 from ventricular tissue prepared from WT and NOX2KO mice with or without 150 nM DGT (N= 4). Data were normalized to control (without DGT) on the same gel. *P<0.05 vs data without DGT.

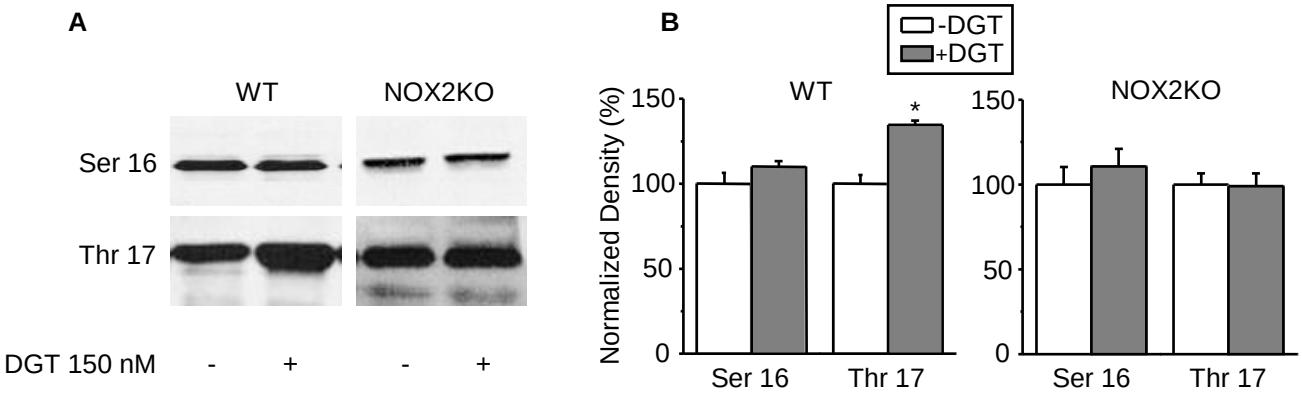

Supplement 5: PLB phosphorylation. A,B representative western blots and normalized pooled data of phosphorylation level at Ser 16 (PKA-dependent) and Thr 17 (CaMKII-dependent) of phospholamban (PLB) from WT and NOX2KO myocytes with or without 150 nM DGT (N= 3). Data were normalized to control (without DGT) on the same gel. *P<0.05 vs data without DGT.

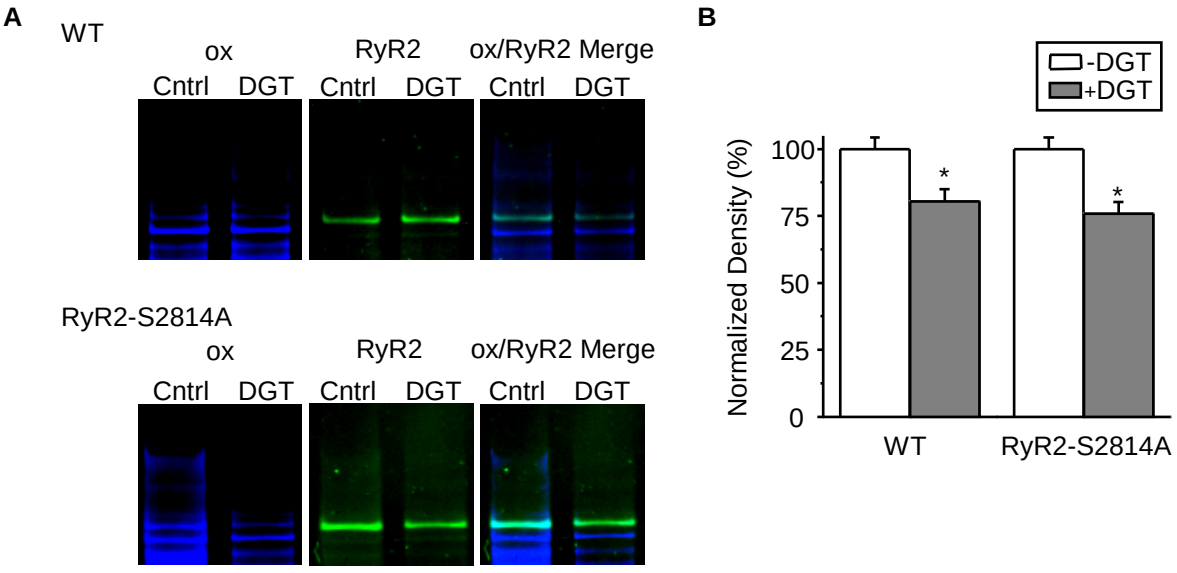

Supplement 6: Oxidation of RyR2 in WT and RyR-S2814A hearts. A, representative simultaneous detection of free thiol and total RyR2 levels in WT and RyR-S2814A hearts. The left panel shows the free thiol content as detected by thiol reactive maleimide-activated DyLight 650 fluorescent labeling in WT and RyR-S2814A samples. The middle panel shows the sequential fluorescent Western detection of total RyR2 by RyR2-specific antibody. The right panel shows the merge of free thiol (blue) and total RyR2 signals (green). **B,** bar graphs of relative free thiol contents normalized to total RyR2 (N= 3 to 4). Data were normalized to control (without DGT) on the same gel. *P<0.05 vs data without DGT.

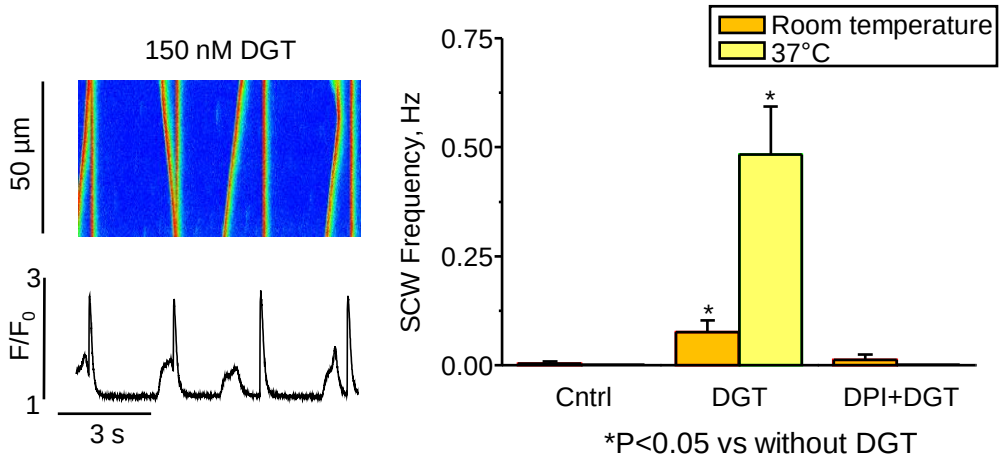

Supplement 7: The effects of DGT and DPI on Ca^{2+} wave frequency at room temperature vs 37°C. Representative line-scan image and time-dependent profile of intracellular Ca^{2+} handling in the presence of 150 nM DGT at 37°C (left), and pooled data for frequency of SCWs in control and in the presence of 150 nM DGT with 50 µM DPI at room temperature and at 37°C (right). The arrhythmogenic effects of DGT were even more pronounced at 37°C than at room temperature and were similarly inhibited by DPI. These results along with those of our biochemical protein phosphorylation- and oxidation assays (fig. 4 and supplemental fig. 5, 6, 7) suggest that our findings are applicable to "physiological" 37°C (N= 4 to 5). *P<0.05 vs data without DGT.